Supplementary Information (SI) for Physical Chemistry Chemical Physics.

Supporting Information

Engineering Berry Curvature and Anomalous Transport via Dimensional Confinement in Correlated Topological Thin Films

Junais Habeeb Mokkath

junais.mokkath@aasu.edu.kw

College of Integrative Studies, Abdullah Al Salem University (AASU), Block 3, Khaldiya, Kuwait

S1. Lattice Geometry and Thin-Film Construction

The correlated Weyl-Kondo thin film considered in this work is constructed from a diamond-derived lattice truncated along the crystallographic z direction. The system consists of N_z atomic layers stacked normal to the z-axis, with open boundary conditions imposed along this direction and full translational symmetry retained in the in-plane x and y directions. This geometry produces a quasi-two-dimensional slab while preserving the essential symmetry and connectivity of the bulk lattice. Each layer contains two sublattices inherited from the diamond structure, and nearest- and next-nearest neighbour bonds are retained within and between adjacent layers. The top and bottom layers define physical surfaces, allowing explicit evaluation of surface localization, surface states, and confinement-induced spectral reconstruction. Periodic boundary conditions in the plane define a two-dimensional Brillouin zone spanned by (k_x, k_y), which is used throughout for electronic-structure and Berry-curvature calculations.

S2. Effective Hamiltonian

The electronic structure is described by a layer-resolved tight-binding Hamiltonian incorporating kinetic hopping, spin-orbit coupling, Kondo hybridization, and Zeeman coupling. The total Hamiltonian is written as

$$H = H_{\mathrm{kin}} + H_{\mathrm{hyb}} + H_{\mathrm{SOC}} + H_{\mathrm{Z}},$$

where each term is defined below.

S2.1 Kinetic hopping

The kinetic term includes nearest- and next-nearest-neighbour hopping on the diamond-derived lattice, preserving time-reversal symmetry in the absence of magnetic fields. The hopping amplitudes are chosen to reproduce a semi-metallic band structure in the unhybridized limit, with bandwidths comparable to those used in previous studies of correlated topological semimetals.

$$H_{\mathrm{kin}} = \sum_{\langle i,j \rangle} \sum_{\sigma} t_{ij}\, c_{i\sigma}^{\dagger} c_{j\sigma} + \sum_{\langle\langle i,j \rangle\rangle} \sum_{\sigma} t_{ij}^{'}\, c_{i\sigma}^{\dagger} c_{j\sigma} - \mu \sum_{i,\sigma} c_{i\sigma}^{\dagger} c_{i\sigma}$$

S2.2 Kondo hybridization

Correlation effects are incorporated at the level of an effective, momentum-dependent Kondo hybridization between itinerant conduction states and localized degrees of freedom. This hybridization generates a renormalized low-energy band manifold characteristic of the coherent Kondo regime. The treatment is static and mean-field-like, appropriate for low temperatures below the Kondo coherence scale, and does not include explicit frequency dependence or dynamical self-energy effects.

$$H_{\text{kin}} = \sum_{\langle i,j \rangle} \sum_{\sigma} t_{ij}\, c_{i\sigma}^{\dagger} c_{j\sigma} + \sum_{\langle\langle i,j \rangle\rangle} \sum_{\sigma} t'_{ij}\, c_{i\sigma}^{\dagger} c_{j\sigma} - \mu \sum_{i,\sigma} c_{i\sigma}^{\dagger} c_{i\sigma}$$

where $c_{i\sigma}$ annihilates an itinerant (conduction) electron and $f_{i\sigma}$ a localized f-electron state

S2.3 Spin-orbit coupling

Spin-orbit coupling is introduced through symmetry-allowed spin-dependent hopping terms with strength λ_{SOC}. This term plays a central role in generating band inversion and nontrivial Berry curvature, and is treated as a tunable parameter throughout the study.

$$H_{\text{SOC}} = i\,\lambda_{\text{SOC}} \sum_{\langle\langle i,j \rangle\rangle} \sum_{\sigma,\sigma'} \nu_{ij}\, c_{i\sigma}^{\dagger} (\sigma^{z})_{\sigma\sigma'} c_{j\sigma'}$$

with $\nu_{ij} = \pm 1$ encoding the (lattice) chirality of the second-neighbor hopping path.

S2.4 Zeeman coupling

An external magnetic field is incorporated via an out-of-plane Zeeman term B_z, which breaks time-reversal symmetry and enables the stabilization of Chern phases in the confined geometry. Orbital magnetic effects are neglected, and the field couples only to the spin degree of freedom.

$$H_Z = \sum_{i} \left[c_i^{\dagger} (\mathbf{B} \cdot \boldsymbol{\sigma}) c_i + g_f\, f_i^{\dagger} (\mathbf{B} \cdot \boldsymbol{\sigma}) f_i \right], \mathbf{B} = (0,0,B_z)$$

S3. Numerical Implementation

All calculations are performed using the PyQUla simulation environment, which provides efficient routines for constructing layer-resolved Hamiltonians, diagonalizing large sparse matrices, and evaluating topological quantities. For each value of $N_z, \lambda_{\text{SOC}}$, and B_z, the Hamiltonian is constructed explicitly in real space along z and transformed to momentum space in the in-plane directions.

Electronic band structures are obtained by diagonalizing the Hamiltonian along high-symmetry paths of the two-dimensional Brillouin zone. Surface-state character is quantified by projecting eigenstates onto the outermost layers. Spin-resolved properties are evaluated from expectation values of the spin operator $\langle S_z \rangle$ in the eigenstate basis.

S4. Berry Curvature and Chern Number Calculations

Berry curvature is computed using a lattice-gauge discretization over a uniform (k_x, k_y) mesh. For a given occupied band n, the Berry curvature $\Omega_n(\mathbf{k})$ is evaluated from overlaps between neighbouring

Bloch states on the discrete momentum grid. The total Chern number is obtained by summing the Berry curvature of all occupied bands and integrating over the two-dimensional Brillouin zone,

$$C = \frac{1}{2\pi} \sum_{n \in \mathrm{occ}} \int_{\mathrm{BZ}} \Omega_n(\mathbf{k}) d^2k$$

To reduce computational cost, Berry-curvature calculations are performed on reduced-thickness slabs N_z^{Berry} that preserve the low-energy topology while minimizing the Hilbert-space dimension. An anomalous-Hall-like response is estimated by integrating the Berry curvature of partially filled bands up to the chemical potential, providing a measure of the intrinsic band-structure contribution to transverse transport in the quasi-two-dimensional regime.

S5. Density of States and Fermi-Surface Calculations

Bulk and surface densities of states are computed by sampling the two-dimensional Brillouin zone on a dense momentum grid and applying Gaussian broadening to the eigenvalue spectrum. Surface density of states is obtained by restricting the spectral weight to the outermost layers of the slab. Fermi-surface contours are extracted at selected energies using iso-spectral tracing routines, allowing visualization of surface-dominated and bulk-like contributions in the confined geometry.

S6. Parameter Sets

Unless otherwise stated, calculations are performed using the following representative parameter ranges:

- Film thickness: 10 to 80 layers
- Spin-orbit coupling: $\lambda_{\mathrm{SOC}} = 0.05 - 0.30$
- Zeeman field: $B_z = 0.0 - 0.40$ (dimensionless units)

These ranges are chosen to span topologically trivial, Chern insulating, and gapless regimes.

S7. Convergence Tests

Convergence with respect to momentum-space mesh density, slab thickness, and energy broadening has been carefully tested. Berry curvature and Chern number calculations were verified against progressively finer (k_x, k_y) grids to ensure stability of the integrated topological invariants. Thickness-dependent trends were confirmed to be robust against changes in numerical parameters and reduced-slab approximations used for Berry-curvature evaluation.

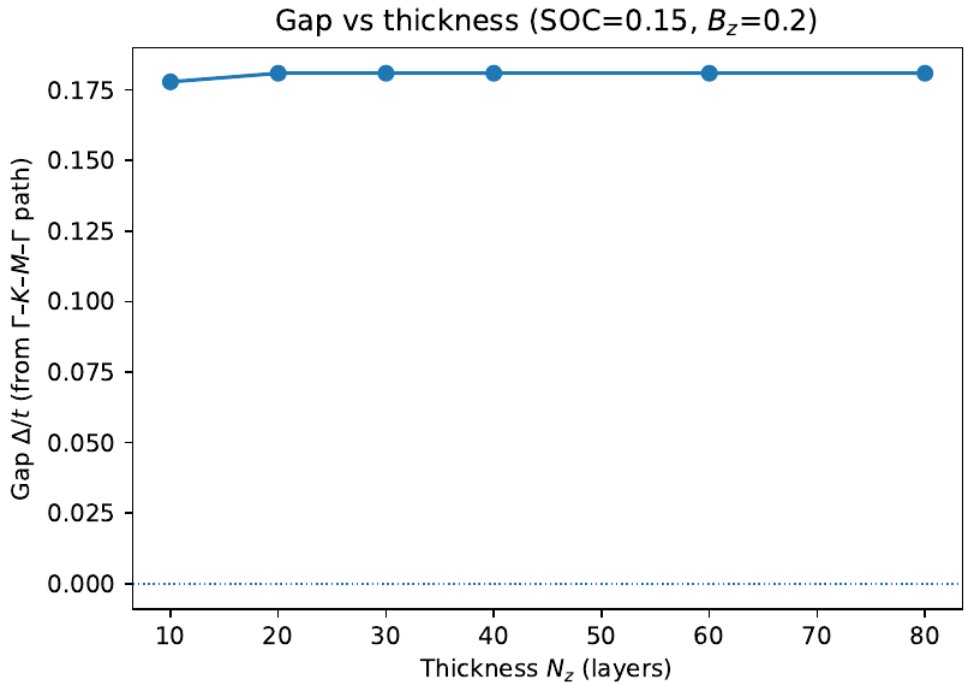

the gap varies non-monotonically with thickness: due to the competition between inter-surface hybridization at small N_z and bulk-like band reconstruction at larger N_z

Table 1: Full list of numerical parameters used in the PyQUla calculations. Energies are reported in units of the nearest-neighbor hopping amplitude t and momenta in reciprocal-lattice units of the underlying lattice convention in PyQUla.

Category	**Parameter (symbol)**	**Value(s) used in this work**
Geometry	Lattice / parent geometry	Diamond lattice (`geometry.diamond_lattice()`)
Geometry	Film construction	Slab via `films.geometry_film(...)`
Geometry	Boundary conditions	Open along z; periodic in-plane (x–y)
Geometry	Thickness (default)	$N_z = 20$ layers
Geometry	Thickness sweep	$N_z \in \{10, 20, 30, 40, 60, 80\}$
Single-particle terms	Energy unit	t (nearest-neighbor hopping amplitude)
Single-particle terms	Strain (directional)	$\varepsilon(\mathbf{r}) = 1 + 0.8\,\lvert z\rvert$ via `add_strain(..., mode="directional")`
Single-particle terms	SOC (Kane–Mele)	$\lambda_{\mathrm{SOC}} = 0.15$ (default) via `add_kane_mele(soc)`
Single-particle terms	SOC sweep	$\lambda_{\mathrm{SOC}} \in [0.05, 0.30]$ (8 points, linear)
Single-particle terms	Zeeman field	$\mathbf{B} = (0, 0, B_z)$ via `add_zeeman([0,0,Bz])`
Single-particle terms	Zeeman (default)	$B_z = 0.2$
Single-particle terms	Zeeman sweeps	$B_z \in [0, 0.4]$ (9 points, linear)
Band structure	Path sampling	`get_bands(nk=NK_BANDS)`
Band structure	Points along path	$N_k = 200$ (`NK_BANDS=200`)
Band structure	Thickness-scan bands	$N_k = 80$ (used inside thickness scan)
Band structure	Spin-resolved bands	`get_bands(operator="sz", nk=200)`
Band structure	Surface-weight bands	`get_bands(operator="surface", nk=200)`
Berry / topology	Berry curvature mesh	`get_berry_curvature()` (default internal mesh of PyQUla)
Berry / topology	Chern number	`get_chern()` (computed from Berry curvature of occupied bands)
Berry / topology	AHC-like integral	$\sum_{\mathbf{k}} \Omega(\mathbf{k})\,\Delta k_x \Delta k_y$ (script-defined normalization)
DOS	Energy window	$E \in [-2, 2]\,t$ (`e_min=-2.0`, `e_max=2.0`)
DOS	Energy grid	$N_E = 400$ (`nE=400`)
DOS	Broadening	$\delta = 10^{-2}$ (Gaussian/Lorentzian per PyQuLa DOS implementation)
DOS	Surface DOS	`get_dos(operator="surface", energies, delta)`
DOS	Bulk DOS	`get_dos(operator="bulk", energies, delta)`
Fermi surface	Target energy	$E = 0$
Fermi surface	Broadening window	$\delta = 0.05$
Fermi surface	k sampling	$N_k = 80$ (`nk=80`)
Parameter maps	Chern map grid	8×9 points in $(\lambda_{\mathrm{SOC}}, B_z)$
Parameter maps	AHC vs B_z grid	9 points in $B_z \in [0, 0.4]$